Constant-pressure molecular dynamics simulations of room-temperature pressure-volume isotherms of Ne and Ar at high densities

1989 J. Phys.: Condens. Matter 1 4885

(http://iopscience.iop.org/0953-8984/1/30/002)

J. Phys.: Condens. Matter 1 (1989) 4885–4894. Printed in the UK

Constant-pressure molecular dynamics simulations of room-temperature pressure–volume isotherms of Ne and Ar at high densities

V Karttunen†, J Ignatius†‡, J Keinonen† and R M Nieminen§

† Accelerator Laboratory, University of Helsinki, Hämeentie 100, SF-00550 Helsinki, Finland

§ Laboratory of Physics, Helsinki University of Technology, SF-02150 Espoo, Finland

Received 30 January 1989, in final form 7 April 1989

Abstract. Constant-pressure molecular dynamics techniques have been used to simulate pressure–volume isotherms of room-temperature Ne and Ar using generally adopted pair potentials. Deviations between the experimental and simulated isotherms are discussed in terms of the repulsive part of the potentials. The relevance of the simulations for the studies of Ne and Ar crystallites in metals has been considered.

1. Introduction

In recent years, observations of the formation of crystalline heavy-inert-gas precipitates in metals [1–6] have stimulated experimental and theoretical studies on the properties of precipitates and gas–metal interfaces [7–16]. These studies have underlined the need to understand the equation of state of inert gases at high pressures from about 2 to about 10 GPa [1, 8, 12]. The strong gas–metal repulsion leads to the segregation of the gas to pressurised 'bubbles', with observed diameters from 10 Å upwards. The density and the structure of the bubble is governed by the interplay between the gas–metal and gas–gas interactions. The recently developed constant-pressure molecular dynamics (CPMD) techniques [17, 18] offer a realistic method for simulating atomic densities, phase diagrams, sizes and growth of the precipitates in different host metals as well as the structures of the gas–metal interfaces. Both the quantitative and qualitative reliability of such studies depend on how accurately the pair potentials assigned for the interactions can describe the equation of state of inert gases.

From an experimental point of view, Ne and Ar are highly suitable gases for the studies of the formation of crystalline precipitates and their physical properties. At room temperature Ne bubbles are liquid [19] in most metals, while Ar precipitates are solid [1, 5, 20]. As a first step in the study of small three-dimensional Ne and Ar crystallites in different metals, we have in the present work simulated the 293 K pressure–volume isotherms of Ne and Ar by CPMD calculations using the pair potential of Ne by Siska and co-workers [21] and of Ar by Ross and co-workers [20]. The Lennard-Jones 6–12 potential often adopted in the literature for molecular dynamics calculations was also

‡ Present address: Department of Theoretical Physics, University of Helsinki, Siltavuorenpenger 20C, SF-00170 Helsinki, Finland.

0953-8984/89/304885 + 10 $02.50

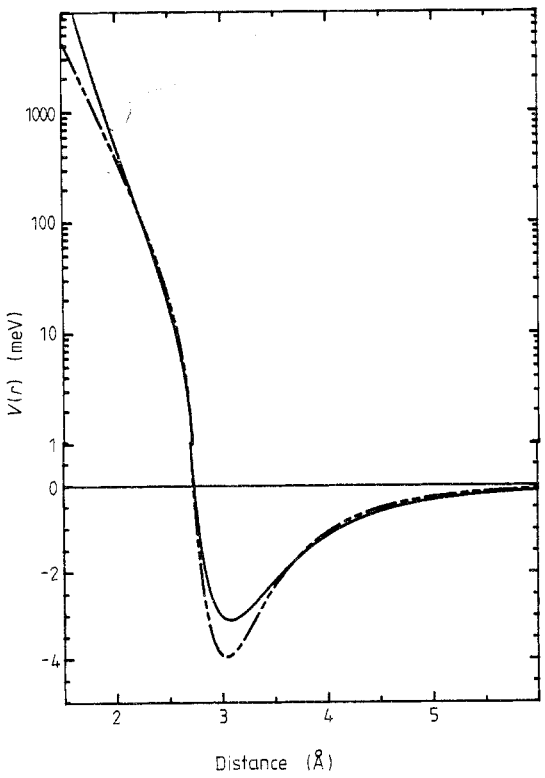

Figure 1. Pair potentials of Ne. Full curve, Lennard-Jones 6–12; chain dotted curve, Siska *et al* [21].

used. In the potential proposed by Siska and co-workers [21] for Ne, the strong short-range repulsion has been reduced by describing it with an exponential term. Several potentials with exponential terms for the repulsion have been reported for Ar (e.g. [20, 22–26]) and used to calculate the 293 K pressure–volume isotherm of solid Ar by the Monte Carlo method [23]. The exponential–6 potential of [20] has produced results closest to the high-pressure data.

In § 2 we briefly describe the simulation techniques. The results are presented in § 3, while § 4 contains a discussion and a summary.

2. Principles of the simulations

The simulations were performed using the constant-pressure molecular dynamics method described by Parrinello and Rahman [18]. This technique, originally proposed by Andersen [17] and further developed in [18], allows both the volume and the shape of the simulation cell to change dynamically. The particle number and pressure are conserved. Apart from a small correction arising from the degrees of freedom of the simulation cell the enthalpy is also conserved.

The basic computational unit cell comprised 864 atoms. Periodic boundary conditions were applied in all three dimensions. Initially, the simulation cell was a cube and the atoms were placed in a FCC array. The random initial velocities of the atoms were chosen to yield 293 K as the temperature of the atom ensemble.

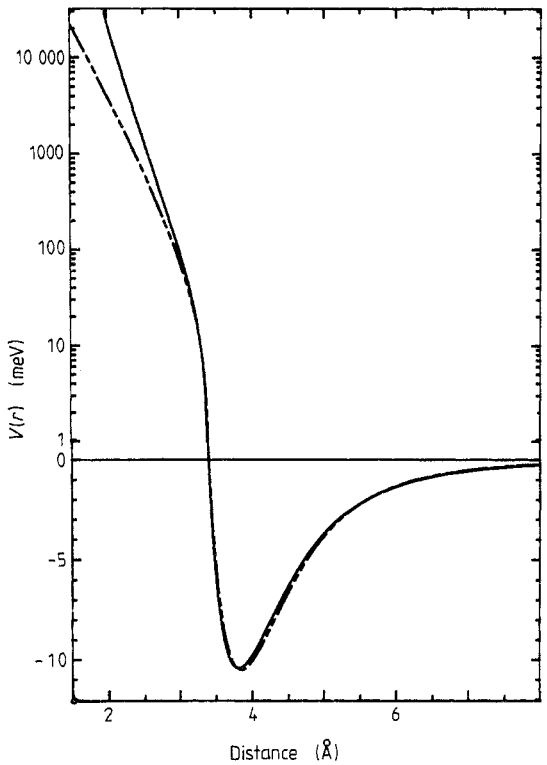

Figure 2. Pair potentials of Ar. Full curve, Lennard-Jones 6–12; chain dotted curve, exp–6 [20].

The equations of motion of the atoms and simulation cell were solved numerically using a predictor–corrector algorithm [27, 28]. A typical time step of $\simeq 10$ fs was repeated 1500 times resulting in a total simulation time of 15 ps. In the simulations at pressures above 25 GPa, the time step was reduced with increasing pressure down to $\simeq 1$ fs. The physical quantities were calculated as mean values between steps 1000 and 1500. The statistical uncertainty of the molar volume values was 0.02–0.1%. In order to reduce the computing time without affecting the final results the temperature was kept constant during the simulation by occasional scaling of the kinetic energy of the particles. The validity of this procedure was based on test runs of 10000 steps where the system had reached thermal equilibrium by the time the scaling was switched off. The difference between the values of molar volume from the short and long simulations was less than 0.2%.

The analytical forms and the parameter values of the pair potentials used are given in the Appendix. The potentials are illustrated in figures 1 and 2. The Ne and Ar potentials were truncated at the distances of 7.5 and 10 Å, respectively. Thus the typical number of neighbouring atoms taken into account was about 150. The truncation of the potential increases the values of the molar volume. At the lowest pressures of 3 GPa (Ne) and 1 GPa (Ar), the systematical uncertainty was estimated to be about 1%. The uncertainty decreases rapidly with increasing pressure, e.g. about 0.1% at 25 GPa (Ar).

The pressure–volume isotherms were calculated over a wide range of pressure from 3 to 300 GPa for crystalline Ne and from 1 to 600 GPa for crystalline Ar. The lower limits correspond to the pressures where room-temperature melting takes place.

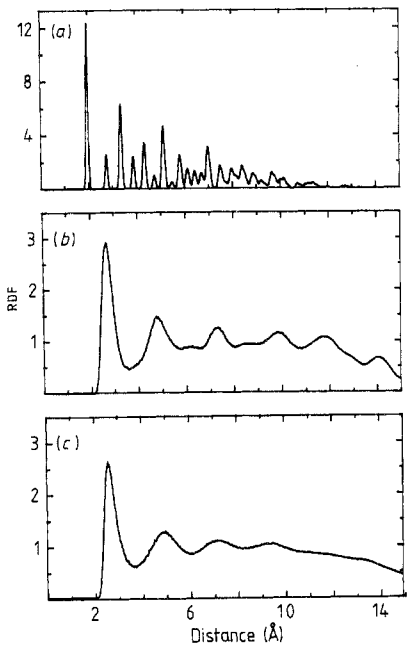

Figure 3. Radial distribution function (RDF) versus distance for Ne at 293 K in the solid phase: (*a*) 300 GPa; (*b*) 3.15 GPa, and in the liquid phase (*c*) 3.00 GPa. Because the RDF has been calculated from the locations of atoms inside the simulation cell, the function does not approach the constant value of 1.0 at distances above 12 Å.

The radial distribution function ((RDF) figure 3) and trajectories (figure 4) of atoms were used to monitor the motion of atoms in the simulation cell and the solid–liquid phase transition. The algorithm for the radial distribution function was adopted from [29], where it is defined as the pair-distribution function. The radial distribution function was calculated from the time-averaged position vectors of the atoms inside the simulation cell. Since the use of the time-averaged position vectors and neglecting the nearest-image convention introduce errors in the RDF values, the radial distribution function determined has merely a qualitative significance.

3. Results

In figure 5 the calculated pressure-volume isotherms at 293 K for crystalline Ne are compared with the experimental data. The data have been measured with diamond-anvil cell and x-ray diffraction techniques from 4.74 GPa (where Ne crystallises) up to 14.4 GPa [19]. The experimental isotherm is reasonably well reproduced by both the Siska and Lennard-Jones potentials. On closer inspection, the molar volume values obtained below ~10 GPa with the Siska potential agree better with experiment than the values obtained using the Lennard-Jones potential. Above 10 GPa the Lennard-Jones potential yields a better agreement. At very high pressures the Lennard-Jones potential can be expected to overestimate the molar volume. The isotherms calculated with the two potentials are estimated to cross at about 30 GPa. The molar volumes calculated for very high pressures (not shown in figure 5) are as follows: 5.65, 3.91 and 3.10 $cm^3\ mol^{-1}$ with the Siska potential and 5.68, 4.19 and 3.50 $cm^3\ mol^{-1}$ with the Lennard-Jones 6–12 potential at the pressures of 25, 120 and 300 GPa, respectively. Experimental data are needed to confirm the validity of the Siska potential at these very high pressures.

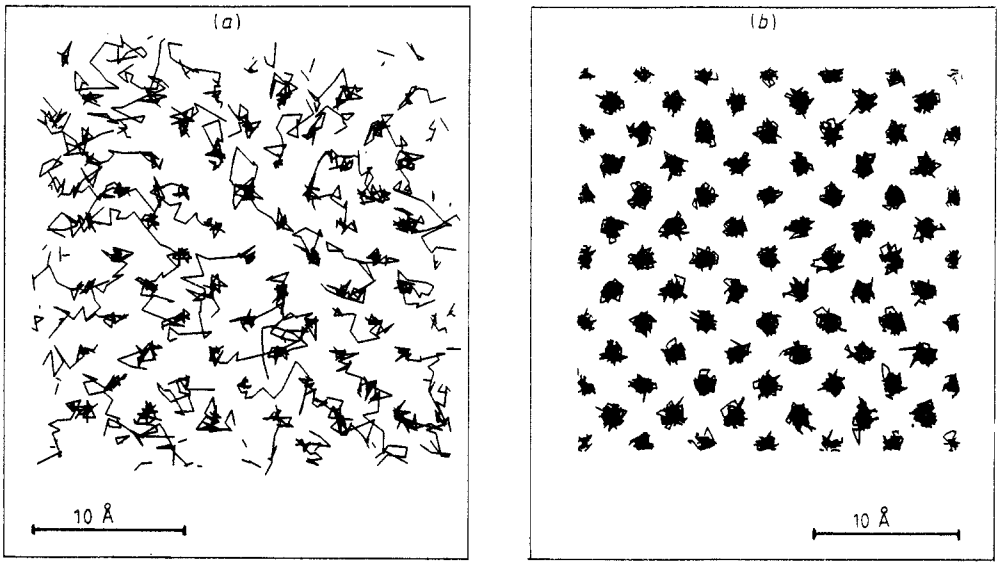

Figure 4. Trajectories of Ne atoms at 293 K; (*a*) in the liquid (3.00 GPa) and (*b*) solid (3.15 GPa) phases.

The experimental isotherm of Ar shown in figure 6 has been measured with diamond-anvil cell and x-ray diffraction techniques at pressures in the range 1.15 GPa (where Ar crystallises) up to 80 GPa [19, 20]. Below about 10 GPa the isotherm is better reproduced by the Lennard-Jones 6–12 potential than by the exponential–6 potential of Ross and co-workers [20]. At higher pressures the values of the molar volume simulated with the exponential–6 potential agree with the experimental data, whereas the overestimation of the molar volume by the Lennard-Jones potential increases strongly with pressure. The molar volumes calculated with the exp–6 potential for the pressures of 150, 350 and 600 GPa (not shown in figure 6) are 6.68, 5.27 and 4.48 $cm^3\ mol^{-1}$ respectively.

The melting pressure of the crystals simulated by CPMD was determined by monitoring the rapid change of the diffusion constant D for self-diffusion, calculated from the basic definition

$$D = \lim_{t\to\infty} (\langle \Delta r(t)^2 \rangle / 6t). \tag{1}$$

The mean square displacement of atoms as a function of time t, $\langle \Delta r(t)^2 \rangle$, is given by the following average

$$\langle \Delta r(t)^2 \rangle = (1/N) \sum_{j=1}^{N} \langle |\bar{r}_j(t+\tau) - \bar{r}_j(\tau)|^2 \rangle \tag{2}$$

where the average is calculated over different values of τ. The melting of the Ne and Ar crystals was estimated to take place at pressures of 3.10 GPa and 0.95 GPa, respectively. Figure 7 illustrates the diffusion coefficient D for different pressures. A diffusion coefficient of $3.7 \times 10^{-5}\ cm^2\ s^{-1}$ has been reported for the atmospheric pressure Lennard-Jones system of liquid Ar at 110 K [30]. The isotherms in the vicinity of the melting for Ne and Ar crystals are shown in figure 8.

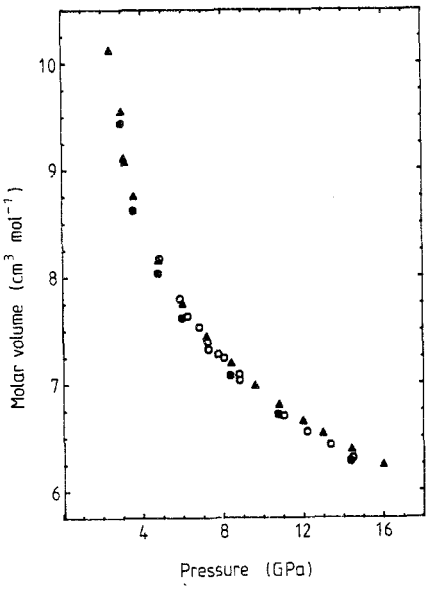

Figure 5. Pressure–volume isotherms of Ne at 293 K. ○, experimental data (after [19]); ●, CPMD (Lennard-Jones 6–12); ▲, CPMD (Siska *et al* [21]).

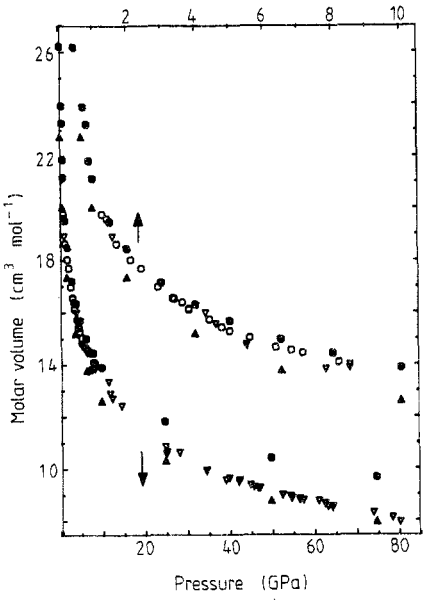

Figure 6. Pressure-volume isotherms of Ar at 293 K. The upper isotherm is in the pressure region 0 to 10 GPa and the lower one in the region 0 to 80 GPa. ○, experiment (after [19]); ▽, experiment (after [20]); ●, CPMD (Lennard-Jones 6–12); ▲, CPMD (exp–6 [20]).

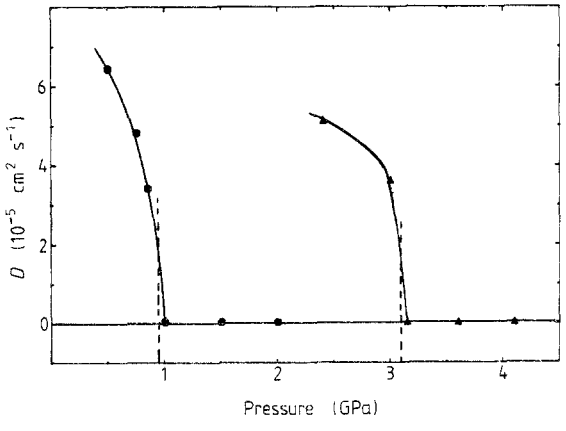

Figure 7. Coefficients of self-diffusion as a function of pressure: ▲, Ne; ●, Ar. The full curves through the points are drawn to guide the eye. The melting pressures are indicated by the broken lines.

4. Discussion

At the high pressures required for the formation of crystalline Ne and Ar, the equation of state is mainly sensitive to the repulsive part of the pair potential. In figures 9 and 10 the Ne and Ar potentials are plotted along with the number of neighbouring atoms at 6.0 and 3.0 GPa, respectively. A stronger repulsion shifts the distribution of neighbouring atoms towards greater separations. At distances below about 2.2 Å, the Lennard-Jones potential of Ne leads to a stronger repulsion than the Siska potential, whereas between

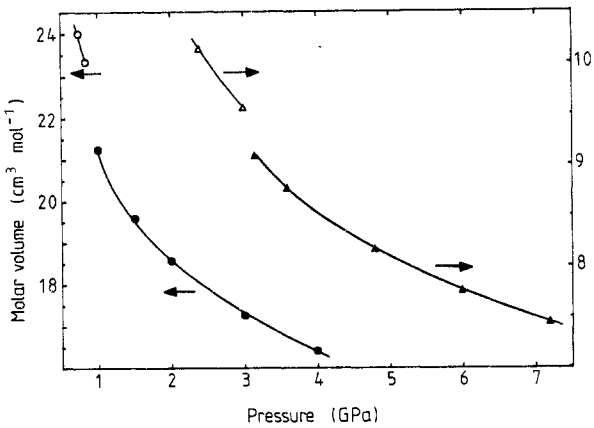

Figure 8. Pressure–volume isotherms of Ne and Ar at 293 K in the vicinity of the melting pressures of Ne and Ar crystals. Ne: ▲, solid; △, liquid. Ar: ●, solid; ○, liquid. The melting can be seen as a rapid increase in the molar volume. The volume values on the left-hand side are for Ar and the right-hand side for Ne.

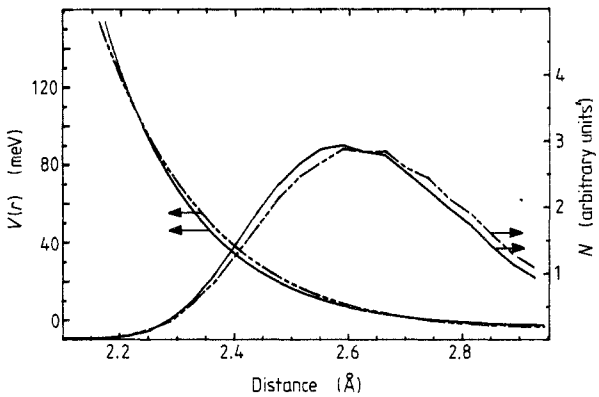

Figure 9. Pair potentials of Ne and the corresponding distributions of neighbouring atoms, N, at 293 K and 6.0 GPa. Full curve, Lennard-Jones 6–12; chain dotted curve, Siska *et al* [21].

2.2 and 2.6 Å the Siska potential is harder (figures 1 and 9). These small differences explain the small but unambiguous differences between the calculated isotherms and experimental data below and above 10 GPa (figure 5). It can be concluded that for the studies of Ne crystallites inside metals, the Siska potential correctly describes the equation of state and hence also the distribution of neighbouring Ne atoms. At distances below about 3.2 Å, the Lennard-Jones potential of Ar has a much stronger repulsion than the exp–6 potential (figures 2 and 10). At pressures below 10 GPa (valid inside Ar crystallites in metals), the Lennard-Jones potential correctly describes the distribution of neighbouring Ar atoms. At pressures above 30 GPa (usually not obtainable in crystallites inside metals), i.e. at distances below about 3 Å, the interaction is better described by the exp–6 than by the Lennard-Jones potential.

A transition of crystalline Ar from the FCC structure to the HCP structure has been predicted to take place below 230 GPa [31]. This transition was not observed in the

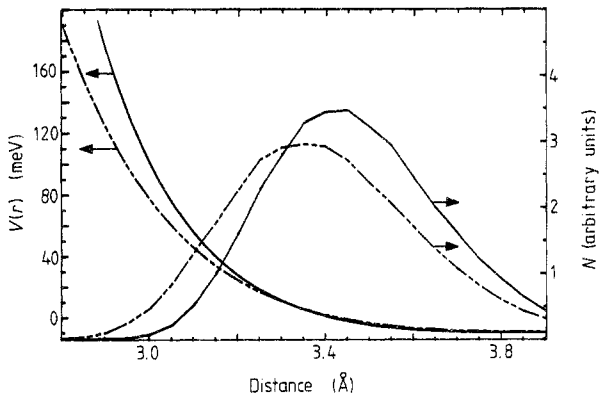

Figure 10. Pair potentials of Ar and the corresponding distribution of neighbouring atoms, N, at 293 K and 3.0 GPa. Full curve, Lennard-Jones 6–12; chain dotted curve, exp–6 [20].

simulations up to 600 GPa. It is evident that at such high pressures inner electron orbitals start to overlap with an effect on the ground-state structure which is not taken into account by the present simulations. In order to study structural phase transitions in small precipitates in future work, both the pair potentials for gas–gas and gas–metal interactions have to be considered.

Tha simulated bulk melting pressures of 3.10 GPa for Ne and 0.95 GPa for Ar crystals are somewhat lower than the respective experimental values of 4.74 and 1.15 GPa [19]. These correspond to the loss of mechanical stability of the crystalline phase as monitored by the self-diffusion coefficient. Considerable hysteresis has been found between melting and freezing points simulated with constant-pressure algorithms (see e.g. [30]). The thermodynamic transition point, in principle obtainable from free-energy estimation, should lie between the two points. This could explain the disagreement between the experimental and simulation results. However, since the growth of the crystallites inside metals, and hence the reduction of the pressure, is expected to be affected by the loop-punching mechanism and damage of the crystalline structure produced in the ion implantation [3–5, 15], the discrepancy is acceptable for the application of the present method in the simulation of precipitates.

In conclusion, the Siska and Lennard-Jones 6–12 potentials for Ne and Ar, have respectively been shown to reproduce well the experimental room-temperature pressure–volume isotherms of these gases. To simulate precipitates of Ne and Ar in metals, effects due to the gas–metal interfaces will also have to be considered.

Acknowledgments

This work was supported by the Academy of Finland.

Appendix

The potentials used in the present work are given below.

Ne (The Siska potential [21])

$$V(r) = \varepsilon f(x) \tag{A1}$$

where $x = r/r_m$,

$$f(x) = \exp[-2\beta(x-1)] - 2\exp[-\beta(x-1)] \qquad 0 < x < x_1 \tag{A2}$$

$$f(x) = b_1 + (x-x_1)\{b_2 + (x-x_2)[b_3 + (x-x_1)b_4]\} \qquad x_1 < x < x_2 \tag{A3}$$

$$f(x) = -c_6 x^{-6} - c_8 x^{-8} \qquad x_2 < x < \infty. \tag{A4}$$

The parameter values used were: $\varepsilon = 3.951$ meV, $\beta = 6.93$, $r_m = 3.03$ Å, $b_1 = -0.7500$, $b_2 = 1.870$, $b_3 = -5.185$, $b_4 = 5.797$, $x_1 = 1.1000$, $x_2 = 1.4000$, $c_6 = 1.282$, $c_8 = 0.278$.

Ar (The exp–6 potential [20])

$$V(r) = \varepsilon\{[6/(\alpha-6)]\exp[\alpha(1-r/r^*)] - [\alpha/(\alpha-6)](r^*/r)^6\} \tag{A5}$$

with the parameter values $\varepsilon = 10.51$ meV, $r^* = 3.85$ Å, and $\alpha = 13.2$.

Ne and Ar (The Lennard-Jones 6–12 potential)

$$V(r) = 4\varepsilon[(\sigma/r)^{12} - (\sigma/r)^6] \tag{A6}$$

where the parameter values were $\varepsilon = 3.121$ meV for Ne and 10.42 meV for Ar, $\sigma = 2.74$ Å for Ne and 3.40 Å for Ar.

References

[1] vom Felde A, Müller-Heinzerling J F T, Phlüger J, Scheerer B, Linker F and Kaletta D 1984 *Phys. Rev. Lett.* **53** 922
[2] Templier C, Jaouen C, Riviére J-P, Delafond J and Crilhé J 1984 *C.R. Acad. Sci., Paris* **299** 613
[3] Evans J H and Mazey D J 1985 *Scr. Metall.* **19** 621
[4] Evans J H and Mazey D J 1986 *J. Nucl. Mater.* **138** 176
[5] Deconninck G and Lefebvre A 1987 *Mater. Sci. Eng.* **90** 163
[6] Evans J H and Hazey D J 1985 *J. Phys. F: Met. Phys.* **15** L1
[7] Finnis M W 1987 *Acta Metall.* **35** 2543
[8] Luukkainen A, Keinonen J and Erola M 1985 *Phys. Rev.* B **32** 4814
[9] Jensen K O and Nieminen R M 1987 *Phys. Rev.* B **35** 2087
[10] Hansen H E, Nieminen R M and Puska M J 1984 *J. Phys. F: Met. Phys.* **14** 1299
[11] Hansen H E, Rajainmäki J, Talja R, Bentzon M, Nieminen R M and Petersen K 1985 *J. Phys. F: Met. Phys.* **15** 1
[12] Donelly S E 1985 *Radiat. Eff.* **90** 1
[13] Frank R C, Rehn L E and Baldo P 1985 *J. Appl. Phys.* **57** 845
[14] Frank R C, McManus S P, Rehn L E and Baldo P 1986 *J. Appl. Phys.* **59** 2747
[15] Keinonen, J, Karttunen V, Räisänen J, Bergmeister F-J, Luukkainen A and Tikkanen P 1986 *Phys. Rev.* B **34** 8981
[16] Keinonen J and Karttunen V 1988 *Phys. Rev.* B **37** 8440
[17] Andersen H C 1980 *J. Chem Phys.* **72** 2384
[18] Parrinello M and Rahman A 1980 *Phys. Rev. Lett.* **45** 1196
[19] Finger L W, Hazen R M, Zou G, Mao H K and Bell P M 1981 *Appl. Phys. Lett.* **39** 892
[20] Ross M, Mao H K, Bell P M and Xu J A 1986 *J. Chem. Phys.* **85** 1028
[21] Siska P E, Parson J M, Schafer T P and Lee Y T 1971 *J. Chem. Phys.* **55** 5762
[22] Barker J A, Fisher R A and Watts R O 1971 *Mol. Phys.* **21** 657
[23] Barker J A 1987 *J. Chem. Phys.* **86** 1509
[24] Aziz R A and Chen H H 1977 *J. Chem. Phys.* **67** 5719

[25] Koide A, Meath W J and Allnott A R 1980 *Mol. Phys.* **39** 895
[26] Parson J M, Siska P E and Lee Y T 1972 *J. Chem. Phys.* **56** 1511
[27] Nordsieck A 1962 *Math. Comp.* **16** 22
[28] Gear C 1971 *Numerical Initial Value Problems in Ordinary Differential Equations* (Princeton: Prentice-Hall)
[29] Rahman A 1964 *Phys. Rev.* A **136** 405
[30] Nosé S and Yonezawa F 1986 *J. Chem. Phys.* **84** 1803
[31] McMahan A K 1986 *Phys. Rev.* B **33** 5344